Design of Complex Biologically Based Nanoscale Systems Using Multi-Agent Simulations and Structure–Behavior–Function Representations

Paul F. Egan
e-mail: pfe@cmu.edu

Jonathan Cagan
e-mail: cagan@cmu.edu

Integrated Design Innovation Group,
Department of Mechanical Engineering,
Carnegie Mellon University,
Pittsburgh, PA 15213

Christian Schunn
Cognitive Program,
Department of Psychology,
University of Pittsburgh,
Pittsburgh, PA 15213
e-mail: schunn@pitt.edu

Philip R. LeDuc
Departments of Mechanical Engineering,
Biomedical Engineering, Computational Biology,
and Biological Sciences,
Carnegie Mellon University,
Pittsburgh, PA 15213
e-mail: prl@andrew.cmu.edu

The process of designing integrated biological systems across scales is difficult, with challenges arising from the modeling, understanding, and search of complex system design spaces. This paper explores these challenges through consideration of how stochastic nanoscale phenomenon relate to higher level systems functioning across many scales. A domain-independent methodology is introduced which uses multi-agent simulations to predict emergent system behavior and structure–behavior–function (SBF) representations to facilitate design space navigation. The methodology is validated through a nanoscale design application of synthetic myosin motor systems. In the multi-agent simulation, myosins are independent computational agents with varied structural inputs that enable differently tuned mechanochemical behaviors. Four synthetic myosins were designed and replicated as agent populations, and their simulated behavior was consistent with empirical studies of individual myosins and the macroscopic performance of myosin-powered muscle contractions. However, in order to configure high performance technologies, designers must effectively reason about simulation inputs and outputs; we find that counter-intuitive relations arise when linking system performance to individual myosin structures. For instance, one myosin population had a lower system force even though more myosins contributed to system-level force. This relationship is elucidated with SBF by considering the distribution of structural states and behaviors in agent populations. For the lower system force population, it is found that although more myosins are producing force, a greater percentage of the population produces negative force. The success of employing SBF for understanding system interactions demonstrates how the methodology may aid designers in complex systems embodiment. The methodology's domain-independence promotes its extendibility to similar complex systems, and in the myosin test case the approach enabled the reduction of a complex physical phenomenon to a design space consisting of only a few critical parameters. The methodology is particularly suited for complex systems with many parts operating stochastically across scales, and should prove invaluable for engineers facing the challenges of biological nanoscale design, where designs with unique properties require novel approaches or useful configurations in nature await discovery. [DOI: 10.1115/1.4024227]

1 Introduction and Motivation

Successful design at the nanoscale ($\sim 10^{-9}$ m) typically requires consideration of mechanical, thermal, and chemical forces that contribute to stochastic behaviors and interactions among system components [1]. The complex system behavior that emerges from component interactions often spans multiple scales, thus resulting in a design space that is difficult to traverse [2]. Solutions to these complex problems often resemble natural system functioning [3], such as the hierarchical organizations of cells and tissues, and there is great potential for engineers to learn from, and utilize, natural systems toward the advancement of nanotechnology [4]. For instance, natural motor proteins [5] have efficiencies much greater than synthetic nanomachines and are therefore often re-implemented in nanotechnologies including responsive materials [6], lab-on-chips [7], and molecular detectors [8].

This paper explores how engineers may design synthetic motor proteins with characteristics targeted for specific nanotechnologies and our approach is a significant contribution toward helping engineers understand and improve the emergent performance of a complex system. Emergence is a crucial mechanism of many complex systems and is often considered unintuitive [2] and difficult to understand [9]. There is much debate on the definition of emergence [10,11], in our context of emergence, we use the definition of *the aggregate system behavior that occurs through collective interactions of system components.*

A domain-independent design methodology is introduced that utilizes multi-agent simulations to model and predict the performance of emergent systems [12,13] and SBF representations to facilitate navigation of the multiscale design space [14,15]. The resulting methodology should enhance an engineer's ability to improve emergent system performance via component alterations. The methodology is tested through a domain-specific application of synthetic myosin protein design. Myosins are one of the most well studied molecular machines, have played significant roles in the emerging field of molecular powered devices [5], and have additional applications in synthetic muscle [16], tissue engineering [17], and disease treatment [18,19]. The exploration of synthetic myosins using formal design methods could also result in the future discovery of novel myosin configurations with unique properties, including those that either do not exist naturally or are undiscovered—the potential of these discoveries is quite feasible

when considering the tremendous rate that novel molecules and functions are being uncovered [20,21].

1.1 Natural Myosin Functionality.

Myosins are essential components for cellular tasks including cytoskeletal scaffolding [22], cellular division [23], and active diffusion [24]. Each task is typically facilitated by a specific class of myosin isoforms [25,26] (isoforms are proteins of the same species with slight structural variations). In this paper, we focus specifically on Myosin II isoforms, the smallest power-producing components in muscle. Figure 1 illustrates four organizational levels of the complex muscular hierarchy, from a complete muscle to an individual myosin. Muscles contain myofibril fibers in parallel and myofibrils are composed of sarcomeres arranged in series, which are the smallest contractile unit of the muscle. Each sarcomere consists of actin protein filaments (filaments at the top and bottom of the sarcomere, as shown in Fig. 1) arranged in parallel with thick filaments that are myosin aggregates (middle filament in Fig. 1).

Myosins operate by cyclically converting the chemical energy of one adenosine triphosphate (ATP) molecule to mechanical energy [27] while powering sarcomere contractions. Contractions among different muscles may vary greatly in terms of force, velocity, and energy performance which is partly influenced by variances in myosin isoforms and their corresponding mechanical and chemical behaviors [28,29]. We define mechanical behaviors as actions explainable in terms of physical forces and displacements, such as how far a myosin moves an actin filament, whereas chemical behaviors are defined as chemical reactions, such as the likelihood of a myosin binding to actin. Both the mechanical and chemical behaviors of myosins are stochastic due to thermal fluctuations. Because thermal fluctuations lead to events that have average outcome values over many trials, their average values may be considered as constants when input as parameter values for predicting the outcomes of mechanical and chemical behaviors at a constant environmental temperature [1]. Although the stochastic nature of the system components at the nanoscale makes each individual myosin's behavior unpredictable, when possibly quadrillions of myosins interact in muscle, a regulated behavior as a whole emerges. Therefore, understanding myosin performance in a multiscale context requires both an understanding of individual myosins and their organization in a system.

1.2 Myosin Complexity.

Although the entire muscular hierarchy forms a single complex system, we argue that even subsystems, such as the configuration of the sarcomere require treatment as a complex system. According to a National Science Foundation workshop on engineering complex systems [2], complex systems consist of a large number of interacting components that may span
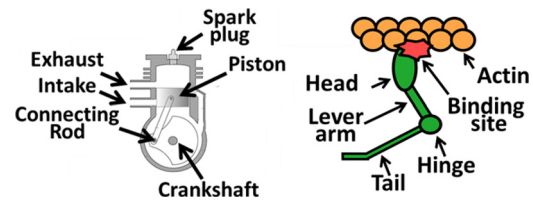

Fig. 2 A schematic a two-stroke motor and a myosin with labeled structures [30]

multiple scales of space and/or time. A sarcomere has possibly 15,000 myosins in addition to other molecules. These entities interact through mechanical and chemical behaviors that require milliseconds, yet enable a contractile event that could span a few seconds.

Additionally, Complex systems also exhibit emergence, namely, new behaviors that result from aggregated behaviors of subsystems [2]. The emergent performance of a contractile event, such as the force and speed of a filament, are enabled by the stochastic behaviors of myosin and actin populations although neither myosin nor actin are individually responsible for the system functioning. To state succinctly: although a sarcomere contracts, myosins and actin do not. A contractile event is an emergent system behavior that arises from a specific organization of myosin and actin. Any force-responsive system utilizing groups of myosins should consist of a similar organization at the myosin and actin level (i.e., myosins stochastically interacting with a travelling filament), thus the design of myosin-based technologies suggests a complex systems approach.

Because of the limitations in human understanding of complex systems, we chose to express myosin systems with a SBF representational scheme, which is considered a language for understanding [15] and designing complex systems [14]. In SBF terminology, *structures* refer to the elements of a system, *behaviors* are the causal chain of mechanisms that allow the structures to achieve their outcome, and *functions* refer to the role an element has within a system. To illustrate SBF and highlight nanoscale design challenges, a well-understood two-stroke motor and a myosin are juxtaposed in Figs. 2–4.

Both motors have similar moving structural components (e.g., the macroscopic crankshaft, connecting rod, and piston resemble the myosin hinge, lever arm, and head in Fig. 2), although a myosin requires a nearby actin binding site to initiate the chemical reactions necessary for subsequent behaviors. Each motor has a series of structural states (labeled images in Fig. 3) where components have varied spatial and temporal relationships that enable subsequent causal chains of behavior (numbered arrows in Fig. 3).
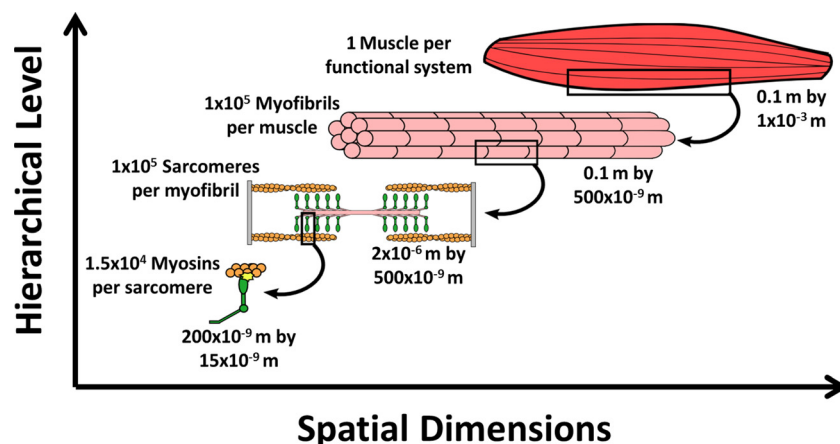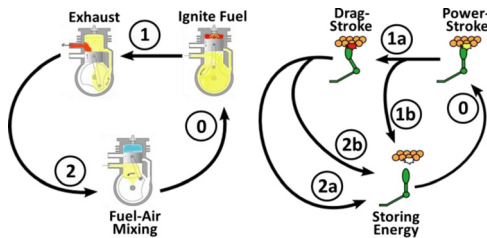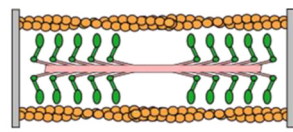

Fig. 1 Schematic of a muscle hierarchy plotted by approximate number of components and approximate physical size (length by height)

Fig. 3 A schematic of structural states and behaviors for a two-stroke motor and a myosin [30]. Each labeled image represents a structural state and each numbered arrow represents a behavior.

Fig. 4 A schematic of the function of a two-stroke motor and a system of myosins [30]

Both motors generate power cyclically; however, a two-stroke motor follows a deterministic set of actions (fuel–air mixing, then fuel ignition, followed by exhausting) while the myosin has multiple possible behaviors that are governed stochastically. Figure 3 will act as a reference in the subsequent discussion that details a myosin's mechanochemical behaviors.

Similar to the macroscopic motor, a myosin must begin its cycle by accepting fuel, but does so by storing energy as mechanical strain through ATP dissociation into adenosine diphosphate (ADP). The myosin has a stochastic chance of attaching to actin based on binding site proximity and filament velocity and therefore remains in its "Storing Energy" state for an indefinite duration. When the myosin attaches to actin, it immediately begins its "Power-stroke" state and produces mechanical force during behavior "1a." While power-stroking, the myosin has a chance of chemically detaching with behavior "1b." Once the myosin has zero strain it begins accumulating negative strain during its "Drag-stroke" state because other motors in the system continue exerting positive force on actin. The myosin remains attached until the strain of the motor head reaches a threshold and mechanically detaches via behavior "2a." The myosin also has a chance of detaching chemically during its drag-stroke as indicated by path "2b."

SBF is a teleological language and therefore a global function is chosen prior to embodying structures and behaviors. For design purposes, only highly likely emergent behaviors of a system require detailed modeling and a designer, if possible, should ensure detrimental emergent behaviors are avoided. For instance, although one two-stroke motor is sufficient for powering a single functional system, one myosin is not sufficient because the actin filament may diffuse beyond a myosin's reach if no other myosins are attached, which is an undesirable emergent behavior. As long as the designer ensures that the system operates with at least one myosin attached at a given time (accomplished by including a significant number of myosins in the system), then explicit diffusion modeling is likely superfluous since it is a highly improbable emergent behavior.

The prediction of emergent behaviors for a particular system embodiment requires an accurate assessment of how varied myosins interact to influence system performance, which we propose is feasible through multi-agent simulations—an approach that has shown success in simulating emergent systems in a number of fields of study [12,13,31]. A multi-agent simulation approach

allows for representing varied individual myosins as computational objects that autonomously interact in a virtual environment. An aggregated measurement of their interactions would describe their emergent performance.

In our approach there are two discrete organizational levels of interest; appropriate SBF terms are used for each level to promote clarity. At the individual myosin level, structure refers to the molecular configuration of a myosin and behaviors refer to a myosin's mechanical or chemical behaviors. We do not go into detail about function at this level, since improving global functioning of the system (i.e., a global objective function) should be the primary concern of a designer, although an implicit assumption of the model is that normal myosin functioning is maintained. At the system level, there is no explicit structure (since structure is a property of individual components); however, the system's organization does influence its functioning (i.e., spatial and temporal relationships among components). When referring to the system behavior, which is the aggregate level behavior of all components in the system, we explicitly state "system behavior," "emergent behavior," or, in the context of designing for a global objective function, "system performance."

Through coupling a clear SBF terminology with the predictive power of a multi-agent simulation, we expect to enable a means for designers to decouple the variances in individual myosin behaviors from system performance, and therefore achieve a deeper understanding of how to reconfigure the system for improved performance. Although our application is focused on systems of synthetic myosins, the combination of SBF and multi-agent simulations is domain-independent, which suggests the methodology is extendible to similar nano- and multiscale complex systems.

2 Background

The first background section focuses on understanding and representing complex systems through SBF representations followed by multi-agent algorithms, synthetic myosin experiments, and mechanochemical modeling approaches.

2.1 Understanding Complex Systems. Complex systems possess specific organizational traits (Sec. 1.2) that differentiate them from merely complicated systems [32]. Studies investigating complex problem solving have shown that complex systems require strategies different from typical problems, with intuitive approaches often outperforming analytical approaches [33]. Several cognitive studies have demonstrated that emergence is a difficult concept to understand, and often causes difficulties in determining how components of a system affect the functioning of the system as a whole [9,15].

Past engineering studies have investigated SBF representations as a language for designing and understanding complex systems, with a recent focus on natural systems at the macroscale [14]. It was found that when students interacted with a multi-agent system that represented a complex aquarium system, they developed a stronger understanding of the system and its interactions [14]. Other investigations have outlined how SBF representations could improve the reasoning process of computational agents during the design process [34].

2.2 Simulating Emergence. Multi-agent simulations are widely used in multiple fields for modeling emergent system behavior via interactions of computational agent populations [12]. Specific applications include social networks [13], ecosystems [14], and molecular systems [35]. In engineering design, multi-agent simulations have been used to model design team interactions [36] and teams of computational agents have optimized designs while searching complex spaces [31,37].

NFSim is an agent-based simulation for determining chemical behaviors among biological components through consideration of
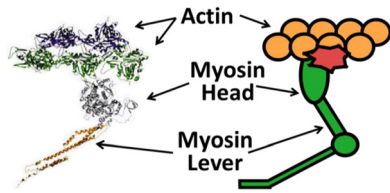
Fig. 5 A schematic of key myosin structures labeled on the molecular representation via X-ray crystallography [25] on the left and an illustration on the right

Fig. 7 A schematic of myosins in a motility assay with actin filament velocity and forces at each binding site indicated

a discrete number of reactants [35]. This contrasts to traditional ways of predicting chemical reactions, which usually assume a large number of reactants enables the consistent functioning of a system. However, these traditional methods often do not provide insights into the component behaviors within a system or their spatial and temporal relationships, which is a strength of agent-based approaches.

2.3 Modeling and Designing Myosins. The swinging lever-arm model is a well-accepted theory for describing myosin behavior [1] and has a strong body of supporting evidence [38–40]. X-ray crystallography in recent years has allowed for a more accurate mapping of key components in the swinging lever-arm model to the molecular structure of myosins such as the myosin head, myosin lever, and actin filament as indicated in Fig. 5.

Structural variations in the myosin head and lever correspond to behavioral differences among myosin isoforms and it is possible to alter these structures artificially to design synthetic myosins with desirable behaviors. Experiments have demonstrated that replacing a myosin lever arm with a similar protein structure of a different length, as shown in Fig. 6(a), affects how far a myosin displaces a filament [41]. It is also possible to swap the head structure, as shown in Fig. 6(b), or alter its molecular structure to modulate a myosin's chemical behaviors [42].

Emergent system performance is commonly measured using motility assays (Fig. 7) where myosins placed on a microscope slide cyclically apply force to actin filaments and the filament velocity is measured. Results from motility experiments have informed analytical and simulation myosin modeling approaches. Common to all models is the need to predict filament velocity by
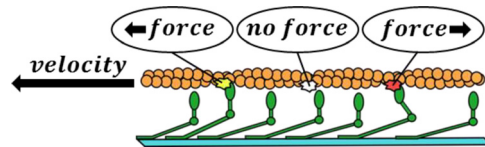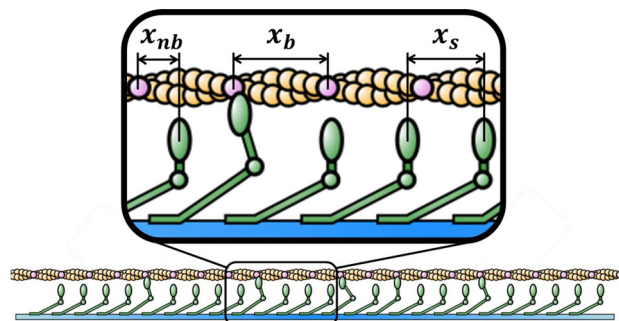
considering the coordinated contributions of multiple myosin motors interacting with actin asychronously. Analytical approaches often utilize differential equations to describe the average behavior of a myosin [1,44–46]; however, assumptions required to generate and solve these differential equations makes model modification and solving difficult. In past work, we utilized an analytic model and found it required modifications to accurately predict how synthetic myosin designs affect emergent performance [47]. Past simulations have tended to concentrate on how myosins are geometrically arranged in muscular components [48,49], with individual myosins following similar assumptions found in the analytical methods. The specific embodiments of myosin systems in these simulations limits their generalization.

Our current choice of a multi-agent simulation has the advantage of modeling stochastic chemical behaviors while also retaining spatial information required for evaluating mechanics that is often ignored in more abstract formulations. Our approach enables tracking the distributions of myosin behaviors and states, rather than assuming their average trends which is common in analytical models. A drawback of the multi-agent simulation is the greater computational effort required to obtain data relative to other methods, although our implementation requires short run-times in practice. Multi-agent simulations are also known for facilitating an intuitive understanding of a system [14] and are generally flexible algorithms that enable quick modification which is beneficial as more refined understandings of mechanochemical dynamics are developed.
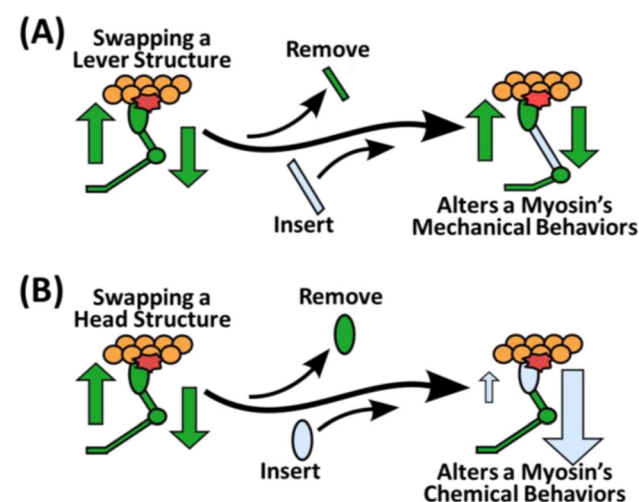
3 Virtual Laboratory Architecture

Our goal is to build a virtual environment that simulates the functioning of a myosin system, with each myosin programmed as an independent computational object (i.e., agent). The virtual environment consists of myosins interacting with a single actin filament and is described in Sec. 3.1. Section 3.2 describes a mathematical description for a myosin's mechanical and chemical behaviors informed by a myosin's molecular structure. Section 3.3 details how myosins are programmed as agents and how they interact with the actin filament. Section 3.4 summarizes the implemented parameter values.

3.1 Virtual Environment. All objects in the virtual environment are constrained to a two-dimensional plane as shown in Fig. 8.

Fig. 6 A schematic of engineering synthetic myosin isoforms with (a) altered mechanical behaviors via lever swapping [41] or (b) altered chemical behaviors through replacement of a myosin's head structure [43] (relative size of up/down arrows represents the magnitude of a myosin's attachment/detachment chemical rate constant)

Fig. 8 Rendering of the virtual environment of twenty five myosins and a long actin filament. Spacing parameters are indicated in the zoomed-view.

Figure 8 also illustrates the computational parameters that represent the spatial relations among components. The environment models myosins that are evenly spaced at x_s length intervals with stationary tails. Myosin heads and lever arms move and interact with binding sites. The distance between a myosin head and the nearest available binding site x_{nb} is allowed to have positive and negative values. All myosins interact with the same infinitely long actin filament with binding sites spaced x_b distance apart and the filament moves at a positive steady-state velocity relative to the myosins (moves to the left in Fig. 8). The infinite filament length assumption ensures that all myosins always interact with the same filament. This virtual setup is equivalent to having actin filaments of equivalent length sliding past myosins one after another. In practice, controlling the system with such precision would be challenging; however, the current level of abstraction enables results that are applicable to a number of differently configured myosin-based technologies.

3.2 Modeling Myosin Structures and Behaviors. A myosin's mechanochemical cycle (Fig. 9(a)) includes three states (Storing Energy, Power-stroke, and Drag-stroke as indicated by illustrations of different myosin structural states and corresponding numbers), three chemical behaviors ("Attachment," "Early Detachment," and "ADP Release," as indicated by the labeled arrows), and one mechanical behavior ("Mechanical Detachment," indicated by a labeled arrow).

During a myosin's Storing Energy state, it has converted an ATP into ADP, is assumed to store the energy as a linear elastic element, and is ready to attach to an actin binding site. Since the filament is moving at a constant velocity, there is a limited amount of time for the myosin to attach to a binding site as it passes. During this time there is a rate constant k_{ON} that represents the probability of attachment (in Fig. 9, the likelihood for a myosin to switch from state "0" to state "1"). If the myosin does not attach, the potential for binding will not occur again until the next site moves into a close proximity. The duration of possible binding time is determined by how long a binding site remains in a myosin's "interaction-zone." The interaction-zone x_z represents how close a myosin head must be to a binding site in order to have a chance to attach. It is assumed that the myosin head in the Storing Energy state is at position δ_+ relative to a myosin's equilibrium position in the environment. The distance δ_+ represents the amount of energy stored as strain in the myosin before attachment. When a myosin binds to actin, the strain e is equal to x_{nb} (when x_{nb} represents the distance of the nearest binding site relative to a myosin head's zero strain position).

Upon attachment, the myosin begins its power-stroke and generates force in the same direction that the filament travels based on its stiffness κ and strain such that the force as a function of time t is

$$f(t) = \kappa \cdot e(t) \qquad (1)$$

While attached, the myosin's strain steadily decreases until it reaches zero. During this time, the myosin has a chance to detach from the filament as governed by the rate constant k_{eOFF} (represented as the Early Detachment behavior in Fig. 9). If the motor remains attached until the strain reaches zero, it switches to its drag-stroke state. During the drag-stroke, the strain increases as the myosin produces force in the opposite direction of the filament velocity. The oppositely strained motor has a structural conformation that enables detachment from the filament when the myosin releases its held ADP. This chemical behavior occurs with frequency k_{OFF} and is referred to as ADP-Release.

If the myosin remains attached without undergoing an ADP release, then its strain continues increasing, thus stretching the myosin arm and head. At some point, this strain will exceed a threshold e_{md} and the myosin will detach mechanically as indicated by the Mechanical Detachment behavior in the diagram. There is no definitive value of e_{md} for natural or synthetic isoforms; however, empirical evidence suggests it is approximately $2 \cdot \delta_+$, which we use for our implementation [50]. Detachment marks the completion of the cycle, with the myosin assumed to remove its ADP and utilize a new ATP. Regardless of detachment behavior, a myosin always begins the next step of the simulation in its Storing Energy state.

3.3 Modeling Myosins as Agents. In multi-agent simulations, agents are independent computational objects that perform actions in a virtual environment according to a set of logical rules programmed into each agent. In our myosin application, the agent logic-circuits shown in Fig. 9(b) represent a myosin's mechanochemical states and behaviors. The agents in our system are not controlled by a manager; each agent makes independent decisions by sensing the environmental conditions, assessing the action to best change the state from its perspective, and then implementing that action. The myosin logic circuits are designed to reflect the physics of a myosin's mechanical and chemical behaviors. Agents are capable of storing data about their own actions, such as their current strain, structural state, the location of the nearest binding site, and their last method of detachment. Emergent system performance is measured by aggregating the data stored by each myosin agent at a particular point in time.

Agents do not interact with one another, but do interact with the same actin filament. During the simulation, first the position of the actin filament is updated along with the position of any myosin heads attached to the filament. Next, all agents (in parallel) determine whether they attach or detach to the filament based on the position of binding sites and their current state. Agents have three possible states corresponding to the structural states of myosin (Storing Energy, Power-stroke, and Drag-stroke as shown in Fig. 9(a)). Depending on an agent's state, the agent follows a set of rules representing the behaviors of attaching and detaching to the filament. These rules are illustrated in Fig. 9(b), with each large block representing a different myosin structural state. An agent's
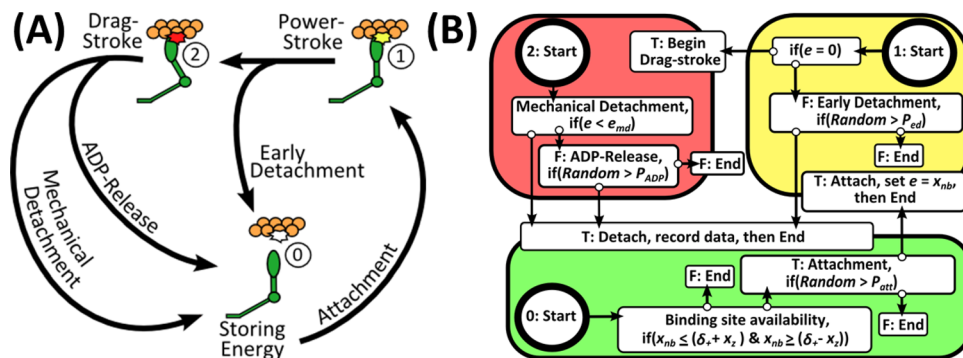

Fig. 9 Modeling myosin agents. (a) A myosin's structural states and mechanochemical behaviors that are (b) simulated by each computational myosin agent's logic circuit.

turn is defined as all of the rules it is allowed to follow during one step of the simulation.

One "Start" circle exists for each state, indicating where a myosin agent begins following rules based on its current state. The agent continues following rules until it eventually reaches an "End" rule that ends its turn. The rules a myosin follows are based on checks that are either deterministically based on the current value of a myosin's strain parameter (such as the Mechanical Detachment check in Fig. 9(b)) or stochastic checks based on rate constant parameters (such as the ADP-Release check in Fig. 9(b)). Stochastic checks are calculated by comparing a random floating-point value between zero and one, labeled as *Random* in Fig. 9(b), and the rate constant of interest. When dT is the time passed during one step of the simulation and k is the rate constant that governs an agent's likelihood of undergoing a chemical reaction during its turn, the probability P that the agent will undergo the reaction is

$$P(k, dT) = k \cdot dT \qquad (2)$$

A spatial step dX is defined as the distance an actin filament moves during one time step of the simulation based on the steady-state filament velocity v such that

$$dT = \frac{dX}{v} \qquad (3)$$

The spatial step and time step should be small enough to accurately capture the physics of the system. For instance, if a myosin has an interaction-zone range of 1 nm, then the spatial step should not be larger than 2 nm. Our implementation uses a spatial step-size of 0.1 nm, and adjusts the time step using Eq. (3). Initially, all agents are set to state 0. Each time a myosin detaches it records its method of detachment (e.g., Early Detachment from Figs. 9(a) and 9(b)). Once every agent has detached (via any method of detachment) at least once, a data point is collected representing that time point in the simulation. Subsequent data points are collected once all agents attach and detach at least one more time.

3.4 Configuring Synthetic Myosin Isoforms. Initially, myosin agents are configured based on values empirically measured for one isoform, thus allowing for later comparisons with the empirical data and an analytical model. Table 1 has a listing of each computational parameter required for the simulation, as described previously, and their values used. The virtual environment parameters are used to configure the spatial relations among myosin agents and the actin filament. The myosin isoform configuration parameters are values that describe each agent and are implemented as an agent reasons through their logic-circuit (Fig. 9(b)) during their turn. For instance, the location of the nearest binding site, the interaction-zone size, and power-stroke distance allows an agent to determine whether it is near enough to a binding site

Table 1   Parameter values used for configuring the virtual environment and myosin isoforms [1]

Parameter	Description	Units	Value
Virtual environment			
x_b	Distance between binding sites	nm	36
x_s	Distance between myosins	nm	29
—	Length of actin filament	nm	∞
Myosin isoform configuration			
δ_+	Power-stroke distance	nm	5
κ	Stiffness	pN/nm	4.1
x_z	Interaction zone	nm	0.5
k_{ON}	Attachment rate	s^{-1}	900
k_{eOFF}	Early detachment rate	s^{-1}	3
k_{OFF}	ADP release rate	s^{-1}	1600

for an attachment attempt. An agent decides whether it is supposed to attach or detach from the filament based on chemical rate constants that are converted into probabilities via Eqs. (2) and (3). An agent's strain is used to determine when it changes from its power- to drag-stroke structural states, when it mechanically detaches, and its force-production via Eq. (1) when data is aggregated.

Parameter x_b is the empirically measured value for the distance between binding sites on actin [1]. The space between each myosin x_s is large enough to ensure noncompetitive binding, which is reflective of muscle functioning. However, *in vitro* approaches have packed myosins on a microscope slide with as little as 10 nm of space separating each myosin [51]. The spring constant κ is inferred from the force a myosin exerts on average at zero velocity [1]. δ_+ represents the linear distance a myosin head moves as the lever arm rotates when storing energy (i.e., the power-stroke distance), and is based on empirical values for the typical power-stroke distance of skeletal myosin [50]. The size of a myosin's interaction-zone is difficult to determine empirically and may fluctuate based on a number of factors such as the stiffness, temperature, and attachment rate of myosins. We assume a small value that is in the acceptable range suggested by empirical evidence [1].

The chemical rates for a myosin detaching during its power-stroke k_{eOFF} and detaching during its drag-stroke k_{OFF} are both empirically informed values. The chemical rate of attaching to actin k_{ON} when a binding site is present is difficult to measure empirically. It is inferred by assuming that a myosin operating at maximum velocity has a cycling rate K_C that is limited by its attachment rate (since the other aspects of the cycle occur with a negligible length of time). The attachment rate constant is then determined by the more commonly measured cycling rate ($\sim$25 s^{-1} for chicken skeletal myosins [1]) and the following relation:

$$k_{ON} = \frac{K_C \cdot x_d}{x_z} \qquad (4)$$

4   Simulation, Experimentation, and Analysis

Initially, the predictions of the multi-agent simulation are validated using values of myosin structures and behaviors that are empirically informed. Next, a virtual experiment is conducted to compare the emergent system functioning of three additional novel isoforms. Since each of these systems always fulfill the same function of powering a motility assay, we refer to varying metrics of system performance to compare how individual myosin designs affect emergent functioning.

Simulations were computed at $\sim$25 GFlops and implemented with Java SE 7 and JavaFX 2.0 with graphical renderings postprocessed (Figs. 8 and 10). All simulations model 25 myosins and collect data at 1000 time points for each steady-state filament velocity (recorded after each myosin completes at least one cycle as described in Sec. 3.3), with most simulations requiring less than a second of computing time. Rendered videos for select simulations are available online as noted in Fig. 10.

4.1   Simulation Validation. To validate the multi-agent simulation, Table 1 values for myosin structures and behaviors were implemented to simulate a "datum" isoform that is compared to empirical results and an analytical model [1]. Renderings of a simulation with a filament velocity of 3 μm/s for 25 myosins are presented in Fig. 10, with the summation of forces from all myosins on the filament indicated by F_{sys}. Initially, all myosins are detached from the actin filament and in the Storing Energy state. In the first panel, a myosin has just attached to the filament and is generating 15 pN of force in its Power-stroke state (as indicated by the size and directionality of the arrow). In the second panel, the myosin has entered its Drag-stroke state while another myosin has attached and is generating positive force. In the third panel, these myosins remain attached as the filament travels and their
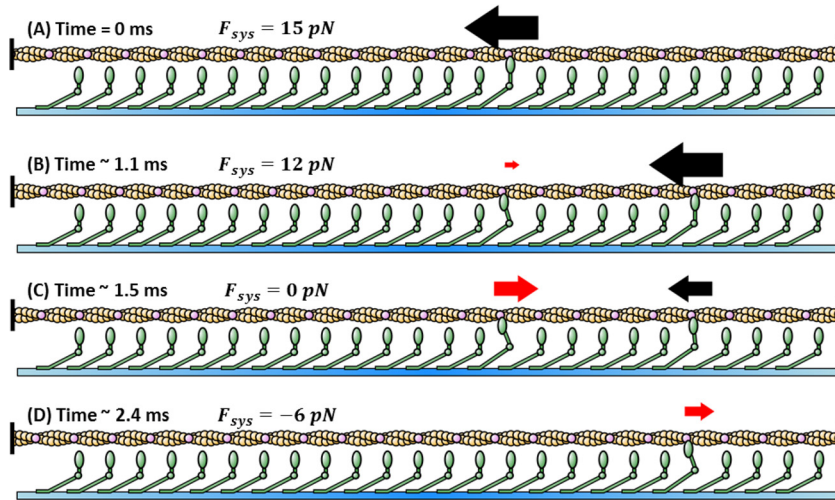
Fig. 10 Renderings of the simulation for four time points when the filament velocity is 3 μm/s. The resulting system force experienced by the filament is indicated for each panel. Simulation renderings are viewable at http://www.andrew.cmu.edu/org/IDIG/SBFSimu.htm.
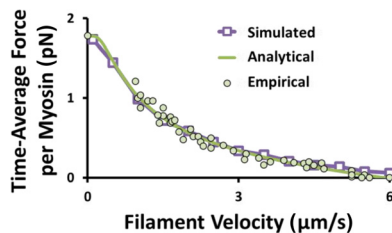
Fig. 11 Time-average force per myosin at different filament velocities using our simulation (squares). These results were compared with previously published analytical and empirical data [1], depicted by lines and circles, respectively.

force generation becomes equal and opposite to one another, thus resulting in zero system force. A myosin's force generation changes because the heads move with the filament, thus decreasing a myosin's strain over time. In the final panel, one motor remains attached in its Drag-stroke state and therefore negative force is exerted on the filament.

The state of the system at each point in time is nondeterministic, so predicting the average emergent system response requires data from many myosins and time points. The time-average force per myosin for a system containing N_m number of myosins with data collected at N_p time points is determined by

$$\langle f(v) \rangle = \frac{1}{N_p \cdot N_m} \sum_{i=1}^{N_p} \sum_{j=1}^{N_m} \kappa_j \cdot e_j(v, t_i) \tag{5}$$
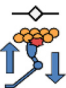
As long as the product of N_m and N_p is large, then the time-average response of different experiments are expected to remain consistent; all of our simulations use 25 myosins with 1000 time points. The aggregate force response was found for thirteen different velocities and the resulting curve is plotted in Fig. 11 along with empirical and analytical data.

The validation demonstrates a close relation between the simulated results and both the empirical data and analytical model [1]. The R squared value is ~0.975 when the analytical curve is considered as the model values for the observed empirical data and the R squared value is ~0.995 when the analytical curve is considered as the model values for the observed simulated data. The hyperbolic relation between force and velocity reflects the force–velocity relationship of muscles at the macroscale [27] and myosins at the nanoscale [52].

4.2 Virtual Experiments With Synthetic Isoforms. A virtual experiment was conducted that simulates four systems populated by synthetic myosin designs with one altered mechanical or chemical behavior parameter (Table 2) while all other computational parameters retain Table 1 values. Extrapolated isoform performance is validated qualitatively in subsequent discussions.

The first system contains myosin isoforms with an increased rate of attachment k_{ON}, thus increasing the likelihood that a detached myosin will attach to the actin filament. The second system has myosins with a decreased k_{OFF} rate constant, thus myosins are more likely to detach chemically during their drag-stroke. The last myosin isoform is designed with a decreased δ_+ distance, which reduces the amount of initial strain a myosin has upon binding and reduces the myosin's power-stroke distance. These parameters are realistic values that future wet-lab experiments could

Table 2 Configuration of synthetic myosin designs used during virtual experiments. Each myosin is identical to the datum isoform of Table 1, except for one altered parameter: The high attachment myosin has an increased k_{ON} rate constant, the low detachment isoform has a decreased k_{OFF} rate constant, and the short stroke isoform has a decreased δ_+ distance.

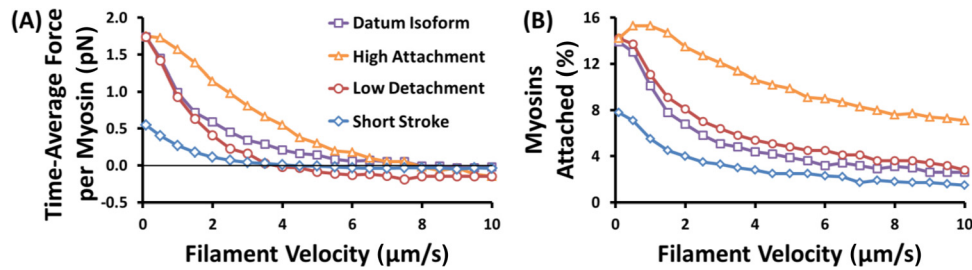| Behavior Parameter	Units	Datum	High attachment	Low detachment	Short stroke
k_{ON}	s^{-1}	900	2700	900	900
k_{OFF}	s^{-1}	1600	1600	800	1600
δ_+	nm	10	10	10	5

Fig. 12 Aggregate performance curves for each simulated system consisting of isoforms from Table 2. (a) The time-average force per myosin and (b) the percentage of myosins in a population that are attached, both plotted against steady-state filament velocities.

replicate [41,42,53] or engineers could use to manufacture myosins for implementation in nanotechnologies.

The multi-agent simulation was run at 21 different velocities between 0.1 μm/s and 10 μm/s with aggregate data for each system determined using the same process from Sec. 4.1. Additionally, the number of myosins attached at each time point was tracked to inform the system's force output [1,54]. Results are plotted in Fig. 12, with each curve representing different systems of myosin isoforms.

Each system has a unique force–velocity and attachment curve. The increased attachment system has higher force values over all velocities in comparison to the datum until its maximum velocity is reached (maximum velocity occurs when $\langle f(v) \rangle = 0$ from Eq. (5)), while the decreased detachment and short stroke systems have lower force values per velocity and lower maximum velocities in comparison to the datum. Additionally, the short stroke system has a lower maximum force. These changes in maximum velocity reflect empirical evidence, thus offering validation for our extrapolated isoform predictions [29,55].

Without considering myosin behaviors, it is difficult to link the variations in molecular structures to system performance. For instance, since only attached myosins produce force it is often claimed that a system with more attached myosins will have higher forces [1,54]. However, in Fig. 11(b) this is only true for the comparison between the increased attachment system and

decreased stroke system to the datum system—the decreased detachment system has a higher percentage of myosins attached than the datum system, yet less force per velocity and maximum velocity. To understand why, we propose an approach using SBF to investigate how individual myosin structures and behaviors relate to a system's functional performance.

4.3 SBF Analysis of Virtual Experiment. To ensure the generalizability of our method, only information about agents that is domain-independent is tracked for the SBF analysis, such as the distribution of structural states and myosin behaviors in the agent population. Three detachment behaviors are tracked: if a myosin detaches early (early detachers), detaches via ADP release (ADP releasers), or detaches due to mechanical strain (mechanical detachers). The percent of myosins that express each of these detachment behaviors at each velocity, referred to as "Behavior Expression," is calculated by determining the total number of myosins that followed a particular behavior and dividing it by the total number of myosins in the system, which is then time averaged.

The behavior expression plots in Fig. 13 demonstrate that the increased attachment and datum systems have identical behavior expression that contrasts with the nearly identical behaviors of the low detachment and short stroke systems, thus reflecting the same relation among systems and their maximum velocity values. The
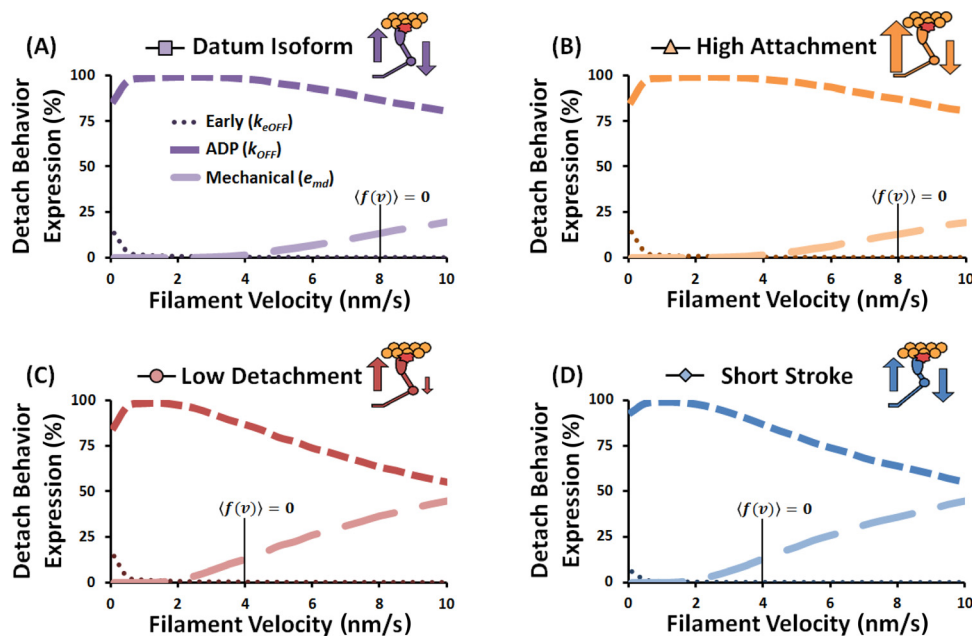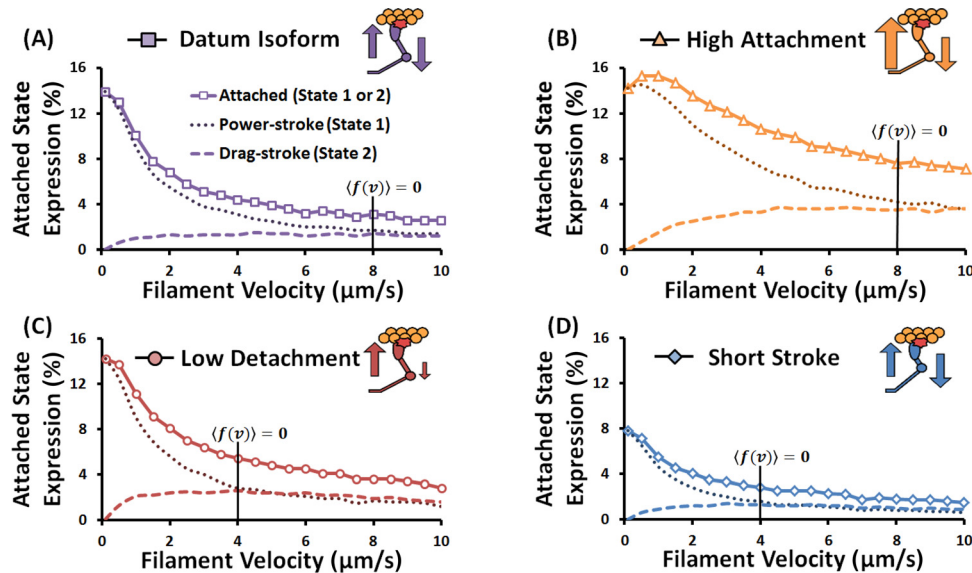

Fig. 13 Percentage of a myosin population undergoing each detachment behavior for each simulated filament velocity. Each plot A-D represents a system consisting of isoforms from Table 2. Each line specifies the percentage of myosins detaching via each mechanism described in Fig. 9, with different dash styles correlating to different detachment behaviors.

Fig. 14 Percentage of a myosin population that are undergoing power- and drag-stroke states, and the total percentage attached for each simulated filament velocity. States correlate to those found in Fig. 9 and are indicated by different dash styles for each line. Each plot A-D represents a system consisting of isoforms from Table 2.

maximum velocities occur near the point when mechanical detachers begin having more prominence in all four systems, thus suggesting a link between the behavior expression in the system and system performance, which can further be linked to individual myosin behaviors. For instance, the decreased detachment system increases the drag-stroke length of a myosin and the short stroke system has myosins that mechanically detach at lower strains (since $e_{md} = 2 \cdot \delta_{+}$, as described in Sec. 3.2), thus providing an explanation for the rise in mechanical detachers at lower velocities. All systems have a low number of early detachers, suggesting that early detachers do not strongly influence system performance, as we have previously demonstrated [56].

The behavior expression plots do not provide insights for why system force–velocity curves differ though, which is necessary for explaining how increasing the number of force-producing motors can lower system force. Therefore, the distribution of structural states in the system was also investigated. The state expression for the power- and drag-stroke states was recorded and generated (Fig. 14) using the same process as Fig. 13. In addition, the summation of the two-states indicates how many motors are attached which reflects the results in Fig. 11.

Figure 14 results demonstrate a unique distribution of states across systems. At the point near maximum velocity, the number of power- and drag-strokers becomes nearly equal meaning the total system force is zero even though myosins are still attached and producing force in equal and opposite directions. When comparing the low detachment system to the datum, it has more motors attached, but the same number of power-strokers and a higher number of drag-strokers. Therefore, it is producing less overall system force due to the increase in attached motors producing negative force, which elucidates our previously counter-intuitive finding that a myosin system with more motors producing force could have a lower system force in comparison to the datum system. The short stroke system, however, has much fewer motors of both power- and drag-strokers in comparison to the datum, which describes its lower force (in addition to its reduced strain).

Additionally, variations in state expression also link to the structural and behavioral variations among isoforms. The decreased detachment population has more drag-strokers because motors spend more time attached to the filament before chemically detaching during their drag-stroke. The increased attachment system increases the total number of motors attached because each myosin is more likely to attach to a binding site on actin as it passes. The short stroke system has myosins with shorter power-stroke distance, causing them to detach mechanically at lower strains and velocities in comparison to the other motors and produce less force in the power-stroke state.

5 Discussion

During the Introduction (Sec. 1.2), we hypothesized that multi-agent simulations could accurately recreate the emergent behavior of myosin systems and that SBF representations could aid a designer's navigation of the complex design space. The discussion will address both of these conditions and also detail how these processes combine to form a domain-independent methodology that is extendible to other complex systems.

5.1 Multi-Agent Simulation Evaluation. The emergent system performance predicted by the multi-agent simulation re-created empirical trends for the natural datum isoform while extrapolated isoforms were validated qualitatively. We found that lowering the detachment rate and shortening the stroke affected the maximum velocity of the system which agrees with empirical findings [29,55]. Furthermore, sources have indicated that the early detachment rate constant should only influence the system at low velocities [1] while mechanical detachers should only influence the system at higher velocities [50]; both of these results were reproduced by the multi-agent simulation [56].

For all designed isoforms, our model predicted similar results to predictions of a past analytical model. Yet our model produces the emergent performance curves through simulation of myosins from the bottom-up (i.e., trends emerge from agent interactions) and does not require *a priori* assumptions of how parameters influence system functioning, as required for analytical modeling where many trends have explicit equations. The agent model enables a designer to reason about how myosin behaviors relate to system performance via virtual experiments, thus providing designers with richer information in comparison to the analytical model. We utilized the multi-agent simulation to investigate only one general type of regulated emergence [11], namely, an emergence that can be controlled through teleological design approaches (in this controlled study, a single actin filament

propelled by a population of myosins). However, due to the flexibility of agent-based models, more specific scenarios of emergence, such as the cooperative dynamics of closely packed myosins competing for binding sites, may be explored with only a few model modifications.

The multi-agent simulation is well-suited for multiscale complex systems in general. For instance, when the force from a myosin is multiplied by the number of myosins in a typical cross-section of muscle [27], approximately $30 \, N/cm^2$ of force is found, which is the typical force output per area of muscles. Therefore, this approach has characterized the aggregate response of a highly complex multiscale system spanning nearly ten orders of spatial scale with a significantly simplified model of the system. The simulation approach also enables designers to configure synthetic myosins and quickly gain feedback of their effects on system performance. Such information is invaluable to the design process and could aid engineers in configuring optimized systems or become the basis of an automated design tool.

5.2 SBF Representations Evaluation. It was difficult to determine how individual myosin variations influenced system performance until the myosin behaviors were investigated with an SBF approach. Specifically, we addressed the counter-intuitive relation that having more motors producing force may actually lower system force when additional motors produce negative-force. These counter-intuitive relations arise in part because myosins have mechanical and chemical behaviors that are both influenced through changing a single molecular structure. For instance, decreasing the detachment rate of a myosin, a chemical behavior, also increases the length of a myosin's drag-stroke, a mechanical behavior. A second example occurs when shortening the stroke because less myosins chemically detach during their power-stroke. SBF representations help designers overcome these difficult couplings through offering multiple routes and means of viewing myosin interactions via their structural states or behavior expression.

There are two general design cases in myosin-based technologies that demonstrate the practicality of SBF reasoning: technologies that always operate at a zero-load case (such as molecular sensors [57]), thus operating at the system's maximum velocity, and technologies that require force-production (such as nanoactuators [16]), thus requiring consideration of the entire force–velocity curve. Both of these systems would have increased performance for synthetic myosins with increased detachment rates and lengthened strokes that raise the force-per velocity and maximum velocity of the systems. However, systems also require consideration of energy performance which is primarily influenced by the myosin attachment rate. Since attachment rate has no effect on the maximum velocity, it would be minimized for the zero-load case but requires more careful consideration among power and energy trade-offs in the force-production cases.

SBF analysis also demonstrates that there are multiple routes of configuring myosins to achieve an identical system performance. For instance, the maximum velocity of systems with myosins of decreased detachment rates and short stroke myosins were identical in our results. Therefore, an engineer may configure a design through altering either parameter, thus motivating a decision based on other factors such as the cost or effort required for generating or manufacturing novel nanocomponents.

5.3 Generalization of Design Methodology. Our methodology was implemented with synthetic myosins, but the pairing of multi-agent simulations and SBF is domain-independent and could apply generally to complex systems. In summary, the methodology consists of five steps that were demonstrated with our synthetic myosin application:

(1) Our methodology applies to systems that consist of many components and possibly have stochastic behaviors across multiple scales; further, the systems must be representable within the SBF framework. In Sec. 1.2, myosin systems were demonstrated to fit these criteria as their structures, behaviors, and functions were described.

(2) A virtual environment was then developed for simulating the emergent system functioning of varied myosins agents and Secs. 3.1–3.4 detailed their implementation. Specifically, the rules for how mysoins interact, how the physics of the system is updated in discrete steps, and what parameters are tunable were all described.

(3) The multi-agent simulation requires validation, as described in Sec. 4.1. Empirical data was used to validate a "datum" isoform and extrapolated myosin designs were validated in Sec. 4.2 with additional details in Sec. 5.1.

(4) Because it is difficult to link how structural changes in system components affects system performance, an SBF analysis was utilized to track the structural states and behaviors of components. In Sec. 4.3, we demonstrated how SBF reasoning could explain the counter-intuitive finding that having more motors producing force actually lowers the system force in some cases.

(5) Finally, the insights gained with the SBF analysis should inform a designer of how to improve system performance via alterations of subcomponents. Section 5.2 demonstrated how two different classes of myosin-based technologies could be improved through linking myosin structural alterations to emergent system performance.

Our analysis requires no further domain-specific information than what was required to produce the multi-agent simulation—all of the design parameter influences were analyzed by tracking the states and behaviors via a SBF representational scheme that could represent components in a number of different systems. Because the methodology requires a teleological identification of an emergent behavior for proper systems functioning, it is best suited for systems where designers are able to configure components that enable a consistent type of emergent behavior. Of interest, there are over twenty more classes of myosins, as well as other species of molecular motors that could initially be explored using this methodology [1,28]. In complex biological systems beyond molecular motor applications, the chemical reactions and simulation framework of the simulation are extendible, but specific agent implementations would vary contextually.

6 Conclusions

Design at the nanoscale often requires consideration of mechanical, chemical, and thermal forces influencing system functioning and systems often contain many components interacting stochastically to produce emergent behaviors. In this paper, a domain-independent methodology for predicting emergent system performance using multi-agent simulations and navigating complex design spaces with SBF representations was presented. Synthetic myosin motor design was investigated as a test case to demonstrate the methodology in a specific biological domain.

One of the greatest benefits of the agent-based approach was the accurate predictions it provided across multiple scales, which considered changes in myosin molecular structures to an entire muscle's force generation. In comparison to traditional methods of myosin modeling, the agent-based approach allows system functioning to emerge from component interactions which offers richer information concerning myosin-to-system level couplings. The approach is also readily extendible to different systems and types of emergent behavior. For instance, the combination of multiple myosin isoforms is common in muscle [28] but is often difficult to explore with traditional experimental and analytical methods. However, the multi-agent implementation could be used to investigate such phenomenon after only a few modifications.

Past SBF studies have focused on macroscopic systems where component behaviors are often considered deterministic. However, at the nanoscale many components act stochastically which

is reflected in our implementation through probabilistic agent actions. We find that even though the actions of each myosin are nondeterministic, the emergent performance of the system has predictable outcomes with respect to varied isoform types. Thus, engineers may design systems with a consistent and high degree of performance at the global level which we demonstrated with our SBF scheme through consideration of two different myosin design applications.

The domain-independent design methodology is extendable to many complex systems in general and has particular strengths in applications where emergent behavior may be highly regulated and in nanoscale mechanochemical applications. The methodology should significantly bolster an engineer's ability to configure multiscale products, especially when considering the complex nanoscale phenomenon our methodology seeks to address. We envision our approach could be extended to reverse engineer myosins that exist *in vivo*, thus aiding the discovery of how specific myosins influence system functioning in nature in addition to facilitating the design of high performance biologically based nanotechnologies.

Acknowledgment

References

[1] Howard, J., 2001, *Mechanics of Motor Proteins and the Cytoskeleton*, Sinauer Associates, Inc., Sunderland, MA.

[2] Guckenheimer, J., and Ottino, J. M., 2008, "Foundations for Complex Systems Research in the Physical Sciences and Engineering, Report From an NSF Workshop." Available at http://math.arizona.edu/~lega/nsf_complex_systems.pdf

[3] Cohen, I., and Harel, D., 2007, "Explaining a Complex Living System: Dynamics, Multi-Scaling and Emergence," J. R. Soc. Interface, **4**, pp. 175–182.

[4] Vattam, S., B. Wiltgen, M. Helms, A. Goel, and J. Yen, 2010, "Dane: Fostering Creativity in and Through Biologically Inspired Design," International Conference on Design Creativity, Kobe, Japan.

[5] Van Den Heuval, M. G. L., and Dekker, C., 2007, "Motor Proteins at Work for Nanotechnology," Science, **317**, pp. 333–336.

[6] Lv, S., Dudek, D. M., Cao, Y., Balamurali, M. M., Gosline, J., and Li, H., 2010, "Designed Biomaterials to Mimic the Mechanical Properties of Muscles," Nature, **465**, pp. 69–73.

[7] Bakewell, D. J. G., and Nicolau, D. V., 2007, "Protein Linear Molecular Motor-Powered Nanodevices," Aust. J. Chem., **60**, pp. 314–332.

[8] Korten, T., Mansson, A., and Diez, S., 2010, "Towards the Application of Cytoskeletal Motor Proteins in Molecular Detection and Diagnostic Devices," Curr. Opin. Biotechnol., **21**, pp. 477–488.

[9] Chi, M., 2005, "Commonsense Conceptions of Emergent Processes: Why Some Misconceptions Are Robust," J. Learn. Sci., **14**(2), pp. 161–199.

[10] Deguet, J., Demazeau, Y., and Magnin, L., 2006, "Elements About the Emergence Issue: A Survey of Emergence Definitions," Complexus, **3**, pp. 24–31.

[11] Bar-Yam, Y., 2004, "A Mathematical Theory of Strong Emergence Using Multiscale Variety," Complexity, **9**(6), pp. 15–24.

[12] Dessalles, J. L., Ferber, J., and Phan, D., 2008, "Emergence in Agent Based Computational Social Science: Conceptual, Formal and Diagrammatic Analysis," Intell. Complex Adapt. Systems, **24**, pp. 1–24.

[13] Gilbert, N., and Troitzsch, K., 2005, *Simulation for the Social Scientist*, Open University Press, New York, NY.

[14] Vattam, S. S., Goel, A. K., Rugaber, S., Hmelo-Silver, C. E., Jordan, R., Gray, S., and Sinha, S., 2011, "Understanding Complex Natural Systems by Articulating Structure-Behavior-Function Models," Educ. Technol. Soc., **14**(1), pp. 66–81.

[15] Hmelo-Silver, C. E., Marathe, S., and Liu, L., 2007, "Fish Swim, Rocks Sit, and Lungs Breathe: Expert-Novice Understanding of Complex Systems," J. Learn. Sci., **16**, pp. 307–331.

[16] Neiman, V. J., and Varghese, S., 2011, "Synthetic Bio-Actuators and Their Applications in Biomedicine," Smart Struct. Syst., **7**(3), pp. 185–198.

[17] Bach, A. D., Beier, J. P., Stern-Staeter, J., and Horch, R. E., 2004, "Skeletal Muscle Tissue Engineering," J. Cell. Mol. Med., **8**(4), pp. 413–422.

[18] Oldfors, A., and Lamont, P. J., 2008, "Thick Filament Diseases," Adv. Exp. Med. Biol., **642**, pp. 78–81.

[19] Armel, T. Z., and Leinwand, L. A., 2010, "A Mutation in the Beta-Myosin Rod Associated With Hypertrophic Cardiomyopathy has an Unexpected Molecular Phenotype," Biochem. Biophys. Res. Commun., **391**(1), pp. 352–356.

[20] Ito, K., Ikebe, M., Kashiyama, T., Mogami, T., Kon, T., and Yamamoto, K., 2007, "Kinetic Mechanism of the Fastest Motor Protein, Chara Myosin," J. Biol. Chem., **282**(27), pp. 19534–19545.

[21] Patino-Lopez, Aravind, G., L., Dong, X., Kruhlak, M. J., Ostap, E. M., and Shaw, S., 2010, "Myosin 1g is an Abundant Class I Myosin in Lymphocytes Whose Localization at the Plasma Membrane Depends on Its Ancient Divergent Pleckstrin Homology (Ph) Domain (Myo1ph)," J. Biol. Chem., **285**(12), pp. 8675–8686.

[22] Koenderink, G. H., Dogic, Z., Nakamura, F., Bendix, P. M., Mackintosh, F. C., Hartwig, J. H., Stossel, T. P., and Weitz, D. A., 2009, "An Active Biopolymer Network Controlled by Molecular Motors," Proc. Natl. Acad. Soc. U.S.A., **106**(36), pp. 15192–15197.

[23] Leduc, P. R., and Robinson, D. N., 2007, "Using Lessons From Cellular and Molecular Structures for Future Materials," Adv. Mater., **19**, pp. 3761–3770.

[24] Leduc, P. R., and Bellin, R. M., 2006, "Nanoscale Intracellular Organization and Functional Architecture Mediating Cellular Behavior," Ann. Biomed. Eng., **34**(1), pp. 102–113.

[25] Tsiavaliaris, G., Fujita-Becker, S., and Manstein, D. J., 2004, "Molecular Engineering of a Backwards-Moving Myosin Motor," Nature, **427**, pp. 558–561.

[26] Hodges, A. R., Krementsova, E. B., and Trybus, K. M., 2007, "Engineering the Processive Run Length of Myosin V," J. Biol. Chem., **282**(37), pp. 27192–27197.

[27] Randall, D., Burggren, W., and French, K., 2001, *Eckert Animal Physiology: Mechanisims and Adaptations*, W.H. Freeman and Company, New York.

[28] Resnicow, D. I., Deacon, J. C., Warrick, H. M., Spudich, J. A., and Leinwand, L. A., 2010, "Functional Diversity Among a Family of Human Skeletal Muscle Myosin Motors," Proc. Natl. Acad. Soc. U.S.A., **107**(3), pp. 1053–1058.

[29] Weiss, S., Rossi, R., Pellegrino, M., Bottinelli, R., and Geeves, M. A., 2001, "Differing Adp Release Rates From Mosin Heavy Chain Isoforms Define the Shortening Velocity of Skeletal Muscle Fibers," J. Biol. Chem., **276**(49), pp. 45902–45908.

[30] Images of Two-Stroke Motor and RC Aircraft are Copyrighted by http://www.RC-Airplane-Advisor.com/ and http://www.RC-Airplanes-Simplified.com/, Images Were Retrieved Mar. 21, 2012 and Modified for This Study.

[31] Campbell, M. I., Cagan, J., and Kotovsky, K., 1999, "A-Design: An Agent-Based Approach to Conceptual Design in a Dynamic Environment," Res. Eng. Des., **11**, pp. 172–192.

[32] Ottino, J. M., 2004, "Engineering Complex Systems," Nature, **427**, p. 399.

[33] Pretz, J., 2008, "Intuition Versus Analysis: Strategy and Experience in Complex Everyday Problem Solving," Mem. Cognit., **36**(3), pp. 554–566.

[34] Gero, J. S., and Kannengiesser, U., 2003, "The Situated Function-Behaviour-Structure Framework," Des. Stud., **25**(4), pp. 373–391.

[35] Sneddon, M., Faeder, J. R., and Emonet, T., 2011, "Efficient Modeling, Simulation and Coarse-Graining of Biological Complexity With NFSim," Nature Methods, **8**(2), pp. 177–185.

[36] Olsen, J., Cagan, J., and Kotovsky, K., 2009, "Unlocking Organizational Potential: A Computational Platform for Investigating Structural Interdependence in Design," ASME J. Mech. Des., **131**(3), p. 031001.

[37] Landry, L., and Cagan, J., 2011, "Protocol-Based Multi-Agent Systems: Examining the Effect of Diversity, Dynamism, and Cooperation in Heuristic Optimization Approaches," ASME J. Mech. Des., **133**, p. 021001.

[38] Schwaiger, I., Sattler, C., Hostetter, D. R., and Rief, M., 2002, "The Myosin Coiled-Coil is a Truly Elastic Protein Structure," Nature Mater., **1**(4), pp. 232–235.

[39] Nath, D., 2010, "Cell Biology: Myosin in Motion," Nature, **468**, p. 43.

[40] Spudich, J., and Sivaramakrishnan, S., 2010, "Myosin Vi: An Innovative Motor That Challenged the Swinging Lever Arm Hypothesis," Nat. Rev. Mol. Cell Biol., **11**(2), pp. 128–137.

[41] Anson, M., Geeves, M. A., Kurzawa, S. E., and Manstein, D. J., 1996, "Myosin Motors With Artificial Lever Arms," EMBO J. **15**(22), pp. 6069–6074.

[42] Murphy, C. T., and Spudich, J. A., 1998, "Dictyostelium Myosin 25–50k Loop Substitutions Specifically Affect Adp Release Rates," Biochemistry, **37**, pp. 6738–6744.

[43] Sweeney, H. L., Rosenfeld, S. S., Brown, F., Faust, L., Smith, J., Xing, J., Stein, L. A., and Sellers, J. R., 1998, "Kinetic Tuning of Myosin Via a Flexible Loop Adjacent to the Nucleotide Binding Pocket," J. Biol. Chem., **273**(11), pp. 6262–6270.

[44] Piazzesi, G., and Lombardi, V., 1995, "A Cross-Bridge Model That is Able to Explain Mechanical and Energetic Properties of Shortening Muscle," Biophys. J., **68**, pp. 1966–1979.

[45] Chin, L., Yue, P., Feng, J. J., and Seow, C. Y., 2006, "Mathematical Simulation of Muscle Cross-Bridge Cycle and Force-Velocity Relationship," Biophys. J., **91**, pp. 3653–3663.

[46] Cuda, G., Pate, E., Cooke, R., and Sellers, J. R., 1997, "In Vitro Actin Filament Sliding Velocities Produced by Mixtures of Different Types of Myosin," Biophys. J., **72**, pp. 1767–1779.

[47] Egan, P., Leduc, P., Cagan, J., and Schunn, C., 2011, "A Design Exploration of Genetically Engineered Myosin Motors," Design Automation Conference, Washington DC.

[48] Tanner, B. C. W., Daniel, T. L., and Regnier, M., 2007, "Sarcomere Lattice Geometry Influences Cooperative Myosin Binding in Muscle," PLOS Comput. Biol., **3**(7), pp. 1195–1211.

[49] Campbell, K., 2009, "Interactions Between Connected Half-Sarcomeres Produce Emergent Mechanical Behavior in a Mathematical Model of Muscle," PLOS Comput. Biol., **5**(11), p. e1000560.

[50] Cooke, R., White, H., and Pate, E., 1994, "A Model of the Release of Myosin Heads From Actin in Rapidly Contracting Muscle Fibers," Biophys. J., **66**, pp. 778–788.

[51] Harada, Y., Sakurada, K., Aoki, T., Thomas, D. D., and Yanagida, T., 1990, "Mechanochemical Coupling in Actomyosin Energy Transduction Studied by in Vitro Movement Assay," J. Mol. Biol., **216**, pp. 49–68.

[52] Ryschon, T. W., Fowler, M. D., Wysong, R. E., Anthony, A. R., and Balaban, R. S., 1997, "Efficiency of Human Skeletal Muscle in Vivo: Comparison of Isometric, Concentric, and Eccentric Muscle Action," J. Appl. Physiol., **83**, pp. 867–894.

[53] Manstein, D. J., 2004, "Molecular Engineering of Myosin," R. Soc., **359**, pp. 1907–1912.

[54] Piazzesi, G., Reconditi, M., Linari, M., Lucii., L., Bianco., P., Brunello., E., Decostre., V., Stewart., A., Gore, D. B., Irving, T. C., Irving, M., and Lombardi, V., 2007, "Skeletal Muscle Performance Determined by Modulation of Number of Myosin Motors Rather Than Motor Force or Stroke Size," Cell, **131**, pp. 784–795.

[55] Uyeda, T., Abramson, P., and Spudich, J., 1996, "The Neck Region of the Myosin Motor Domain Acts as a Lever Arm to Generate Movement," Proc. Natl. Acad. Sci. U.S.A., **93**, pp. 4459–4464.

[56] Egan, P., Leduc, P., Cagan, J., and Schunn, C., 2012, "Design of Complex Nano-Scale Systems Using Multi-Agent Simulations and Structure-Behavior-Function Representations," International Conference on Design Theory and Methodology, Chicago IL.

[57] Agarwal, A., and Hess, H., 2010, "Biomolecular Motors at the Intersection of Nanotechnology and Polymer Science," Prog. Polym. Sci., **25**, pp. 252–277.